First publ. in: Brain Topography 7 (1995), 4, pp. 275-282

The Separation of Overlapping Neuromagnetic Sources in First and Second Somatosensory Cortices

T. Elbert*, M. Junghöfer*, B. Scholz#, and S. Schneider#

Summary: In response to a somatosensory stimulus, two cortical centers in each hemisphere produce neural mass activity large enough to be detected with electric (EEG) or magnetic (MEG) measurements. Both the primary somatosensory cortex (S-I), located in the postcentral sulcus and in the depths of the central sulcus, as well as the secondary somatic sensory cortex (S-II), lying in the upper bank of the Sylvian fissure, respond within the first 100ms such that the two activities overlap in time. We demonstrate that this overlap can be disentangled using a MUSIC-type approach, as suggested by Oppelt and Scholz. It needs no a priori information about the sources. As the results show, there are several instances in time in which only one of the two centers (SI, SII) is active. It is only for these time segments that a single moving dipole yields meaningful results. Such time intervals occur during the upstroke of the late component around 60 ms (only SI activity) and during the down-stroke around 120 ms (only SII activity). In these time intervals the activity of one of the somatosensory areas is still large enough, while the other center is not yet or is no longer active.

Key words: MEG; Somatosensory cortex; Source modeling; MUSIC; Event-related field.

Introduction

The primary somatosensory cortex (S-I) is located in the postcentral sulcus and in the depths of the central sulcus. Lateral and somewhat posterior to S-I is the secondary somatic sensory cortex (S-II), lying in the upper bank of the Sylvian fissure. As it has been shown, both in electrophysiologal studies in animals carried out since the late thirties (Marshall et al. 1941) and in invasive investigations in human patients (Penfield and Rasmussen 1950), the SI and SII are somatotopically organized. The measurement of magnetic fields resulting from thousands of cells and spanning several mm^2 of neuronal mass activity permits the exact localization of the cortical somatosensory map in a completely noninvasive manner (Hari et al. 1993; Hari et al. 1991; Elbert et al. 1994; Yang et al. 1993). The MEG is particularly sensitive to the activity in the fissural cortex in area 3b, since this activity generates current dipoles which are more or less tangentially oriented to the surface of the head.

*Institute for Experimental Audiology, University of Münster, Germany.

#Medical Engineering Group, Siemens AG, Erlangen, Germany.

Accepted for publication: January 20, 1995.

Research was supported by the Deutsche Forschungsgemeinschaft (Klinische Forschergruppe für Biomagnetismus und Biosignalanalyse). We would like to thank Schwind Medizin-Technik, Erlangen for providing the stimulation unit.

Correspondence and reprint requests should be addressed to Prof. Dr. Thomas Elbert, Postfach 5560/D23, D-78434 Konstanz, Germany.

The simplest and, if adequate, most reliable way of source modeling is to model the total activity of all neurons at a given instant in time as a single equivalent current dipole (ECD). The ECD-model, however, will only produce reasonable locations for a particular activity if this activity is focal, i.e., spatially confined to a relatively small region of the brain. For magnetic fields and electric potentials resulting from sensory stimulation such an assumption holds true, if at all, only for short time segments of the total evoked response. Responses evoked by somatosensory stimulation are a perfect example to illustrate the problem. In response to median nerve stimulation, S-I and S-II will be activated in an overlapping manner and simultaneously in both hemispheres. The goal of the present study was to evaluate a recently proposed localization procedure suggested by Oppelt, Scholz and colleagues (Oppelt et al. 1993; Scholz and Oppelt 1992, 1995) which allows the separation of the sources without any a priori assumption about the source locations. With this procedure, the overlapping temporal activation of the two somatosensory fields can be disentangled and activational patterns can be specified. This will also allow the identification of time segments during which the single ECD-model is valid.

This approach is related to another multidipole localization procedure which has been suggested by Mosher et al. (1992). The latter, a special case of the MUltiple SIgnal Classification (MUSIC) method, is called MEG-MUSIC method. Both methods assume that the source activities related to different locations evolve independently in time and that the source locations to be

determined are stationary in time. However, the basic equations used for localization differ between the two approaches. In the presently used method, the localization equation is mathematically simpler and can be solved explicitly. Thus, at least 30% less computing time is needed than in the MEG-MUSIC method. Additionally, the algorithm of Oppelt and Scholz does not require any assumptions on the orientations and the strengths of the dipole moments. A common feature of both procedures is that the dipole locations are found by scanning the volume-of-interest (VOI) on a sufficiently fine grid.

Mosher et al. have shown that, in general, procedures based on Principal Component Analyses will fail, whereas MUSIC-type methods seem to be more promising. In a report by Hari and colleagues (Hari et al. 1993; Hari et al. 1991), S-I and S-II locations have been identified by both the single ECD-model and Mosher's MUSIC-approach, in one case. The present evaluation adds another case which is cross-validated in itself by comparing ipsi- and contralateral sources.

Method

Subject and procedure

The MEG was recorded from a right-handed healthy 27-year-old male subject, in separate runs from both hemispheres. Using an electrical stimulator (Lucius and Baer GmbH) constant current pulses of .5 ms were applied to a dorsal location in the center of the right hand at a constant rate of .95 Hz (Inter stimulus interval 1.052 s). The current was applied by means of a subcutaneous needle electrode, with a ring reference around the wrist. After determining the sensory and the pain threshold, the stimulus intensity was set just below the pain threshold (at 1.5 mA). In order to minimize stimulus artifacts, the polarity was alternated from trial to trial. (Since the analyses for the separate current polarities produced the same results, only the results for averages across both polarities are presented here.) A total of 500 trials was presented per run.

Recordings

Using a 37 channel biomagnetometer (Siemens Krenikon^{TM}, Schneider et al. 1990), magnetic fields were recorded from 35 locations centered either over C3 (left hemisphere) or C4 (right hemisphere), i.e., contralateral and ipsilateral to the site of stimulation. The stability of the subject's position was assured by fitting the subject's face into an individually casted plaster mold which was mounted in a fixed position relative to the sensor array. The mold fitted tightly around the eye-balls, preventing blinks and eye-movements, and had holes to allow normal breathing. Recordings were carried out in a magnetically shielded room. MEG channels were amplified from .016 to 250 Hz (10 s time constant) and sampled at a rate of 1 point per ms.

In the Siemens system, the detection coils are hexagonal in shape, arranged like a honeycomb, in a circular array on a planar surface. In this way, the available sensor area is maximized. The distance between the center of two adjacent coils is 2.7 cm. Sensors are configured as first-order axial gradiometers with a baseline of 7.0 cm. The construction as a foil-system warrants optimal planarity between the two coils of the gradiometer.

The occurrence of R-waves was detected from ECG recordings, and this information was used to trigger averages in the MEG-channels which were then used to correct for cardiac artifacts according to (Abraham-Fuchs et al. 1992). The position of the head and of anatomical landmarks (nasion, preauricular points of the left and right ears, inion and vertex) were identified prior to the MEG-measurement using an Isotrak^{TM} 3D-digitizer (Pholemus Navigation Sciences, Colchester, Vermont, U.S.A.).

Sagittal MR images were obtained on a Siemens Magnetom Impact 1.0 T system. T2_weighted gradient-echo sequences were used (slice thickness 5 mm, 21 slices; recording matrix 256x256 pixels, field of view 240x240 mm^2, TurboGradient Spin-Echo sequence). The same anatomical landmarks used to create the MEG head-based 3D-coordinate system were visualized in the MR images by affixing capsules filled with a solution which produces a high contrast in the MRI to these points. The MEG source locations were converted into pixels and slice values using the MRI scaling factors and inserted onto the corresponding MRIs. For the purpose of constructing the present two figures, the ECD locations of interest were projected onto one MRI slice to allow comparisons between locations.

Analysis of the Event-Related Magnetic Field and Method of source localization

Trials were visually inspected and excluded from the analysis if there were any obvious artifacts. This left an average of 430 trials from the original 500 trials. These trials were corrected for MCG-contamination and then averaged. The offset was removed using a 80ms baseline which spanned the interval from -100 to -20 ms prior to stimulus onset. The interval from 15 to 526 ms (512 pts.) was considered for analysis.

Source localization algorithms from MEG data require model assumptions for the head and for the bioelectric sources in the brain. The head was considered to be a spherical volume conductor with a radially dependent

conductivity distribution. The sources, which were assumed to be focal, are described as pointlike current dipoles. They are characterized by their positions and their dipole moments. The dipole position corresponds to the site of the activity center and the dipole moment vector, i.e., its orientation and strength, describes the activity.

The biomagnetic somatosensory data evaluated in this work were expected to be generated by simultaneously active current dipoles. In order to localize the sources with overlapping activities we used a recently developed multidipole localization algorithm (Scholz and Oppelt 1992, 1995; Oppelt et al. 1993). In this MUSIC-like localization procedure we do not need any a priori information about the sources, like their locations or their activities. However, as in the MEG-MUSIC method (Mosher et al. 1992), the linear independence of the time evolution of the overlapping activities is required. This means that the time behavior of each dipole moment vector has to be different.

The method presented uses the time evolution of the spatial data, i.e., of the magnetic field values recorded simultaneously at the M sensor positions. The number of independently evolving source activities, i.e., of dipole moment components, is obtained from the singular value decomposition (SVD) of a spatio-temporal data matrix. This is a $M \times J$ matrix, where M denotes the number of sensors and J the number of measurement time instances. The j-th column vector denoted by $\underline{B}j$ contains the M magnetic field values $B(t_j, \vec{r}_1) \ldots B(t_j, \vec{r}_M)$ measured at the sensor positions $\vec{r}_1, \ldots, \vec{r}_M$ at time t_j. The SVD for the m_j-th matrix element reads

$$B(\vec{r}_m, t_j) = \sum_{n=1}^{N_s} s_n u_n(\vec{r}_m) v_n(t_j) \quad N_s = \min\{M, J\} \tag{1}$$

The terms in the sum of (1) are ordered according to the descending magnitude of the singular values $s_n n = 1, \ldots, N_s$. The numerically significant singular values are related to the independent dipole moment components which contribute significantly to the signal. The residual singular values are determined by noise. They generate the nearly flat part of the singular value spectrum. In the next section this is illustrated by examples from phantom and real data.

The $u_n, \vec{r}_1, \ldots, u_n(\vec{r}_M)$ are the components of a M dimensional singular vector $\underline{u}_n$ of the data matrix. It depends only on sensor positions and, therefore, can be displayed like a field map. Singular vectors corresponding to the significant singular values exhibit an increasing multipolar structure with an increasing value for n. The residual singular vectors have a random structure due to noise. The first singular vectors are called "eigenmaps" for obvious reasons.

For each of the dipoles with overlapping, linear *independent* activities, a time independent single dipole equation can be derived from (1) (Scholz and Oppelt 1995). This equation arises by considering the time averaged contribution of each source

$$\sum_{n=1}^{N_{sig}} C_n(\vec{r})\, \underline{u}_n = \underline{\vec{L}}(\vec{r}) \cdot \hat{d}, \tag{2}$$

where N_{sig} is the number of significant singular values.

The left side of equation 2 is a linear combination of eigenmaps which is dependent on the dipole position (denoted by the vector $\vec{r}$). The right-hand side describes the magnetic field values at the M sensor positions due to a current dipole at location $\vec{r}$. It is expressed by the corresponding lead field vector $\underline{\vec{L}}(\vec{r})$ and its time averaged, normalized moment vector $\hat{d}$. The lead field is a vector in the ordinary three dimensional space, indicated by the *arrow*, and a M dimensional vector in the data space, denoted by the underline as in the case of the eigenmaps.

Equation 2 represents a system of M equations, with one equation for each sensor. It has $N_{sig} + 1$ unknowns in the case of the sphere as head model. The unknowns are the N_{sig} coefficients c_n and the angle which describes the orientation of $\hat{d}$ in the plane tangential to the dipole position vector. At any point in space the unknowns can be calculated explicitly in a least squares sense.

For noiseless data, the M equations are completely consistent, i.e., they are exactly satisfied, if the dipoles are at their true locations. For data with noise the inconsistency of these M equations can be minimized. The locations of the minima of the corresponding cost function are identified as dipole locations. Thus, the dipole positions can be found by scanning the volume of interest on a sufficiently fine grid. The multidipole search has been transformed to a successive search for single dipoles by means of (2).

The analysis of an electrophysiological process requires the knowledge of the time behavior of the dipole moments. At each time instant t_j the N dipole moment vectors $\vec{d}(t_j, \vec{r}_k)$ at the positions $\vec{r}_1, \ldots, \vec{r}_N$ determine the M magnetic field values contained in the data vector $\underline{\vec{B}}_j$. Defining a multiple moment vector t_j at time by

$$\underline{d}_j = \begin{pmatrix} \vec{d}(t_j, \vec{r}_1) \\ \cdot \\ \cdot \\ \cdot \\ \vec{d}(t_j, \vec{r}_k) \end{pmatrix} \tag{3}$$

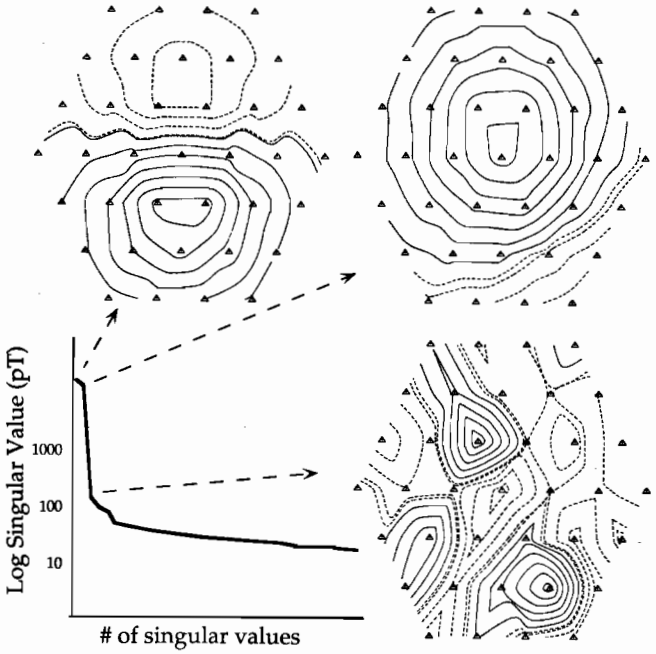

Figure 1. Singular value spectrum (lower left) and first three eigenmaps for the recordings from the phantom head. In this case, the third eigenmap can easily be identified as a noise map.

the relation between the data at time t_j and the moments is

$$\underline{B}_j = L\,\underline{d}_j \tag{4}$$

In the spherical volume conductor model the matrix L is a $M \times 2N$ lead field matrix. It is given by the lead fields belonging to the M sensors and the N current dipole locations.

$$L = \left(\underline{\vec{L}}^T(\vec{r}_1), \ldots, \underline{\vec{L}}^T(\vec{r}_N)\right) \tag{5}$$

where the $M \times 2$ submatrices are given in terms of the spherical lead fields components

$$\underline{\vec{L}}^T(\vec{r}) = \left(\underline{L}_\vartheta(\vec{r}), \underline{L}_\varphi(\vec{r})\right)$$

The dipole moments $\underline{d}_j$ at t_j time are obtained by inverting equation 4. This is done by means of the generalized or Moore-Penrose inverse L^+ for overdetermined systems of equations, see e.g., Lawson et al. (1974).

$$\underline{d}_j = L^+\,\underline{B}(t_j) \qquad L^+ = \left(L^T L\right)^{-1} L^T \tag{6}$$

The solution of equation 6 for consecutive times yields the time behavior of the dipole moments at the localized positions. Equations 3 to 6 show that no assumptions with respect to the dipole moments, i.e., the source activities, were made.

Phantom Model

In order to evaluate the described procedure and to test the source model resulting from the real data, a data set was gained using simultaneously active sources within a phantom head. The phantom consisted of a glass sphere filled with physiological saline solution. The dipolar sources within the phantom were configured to match the expected S-I and S-II locations. The two dipoles were activated simultaneously with sinusoidal variations of 9.5 Hz and a phase delay of 90° between the different sources.

RESULTS

Phantom data

The singular value spectrum of the phantom data is presented in figure 1, together with the first three eigenmaps. There is a clear jump between the signal and noise part of the spectrum, i.e., from the second to the third value. This drop becomes increasingly reduced when more and more noise is added to the signal. As long as the singular values related to dipole moment components are above the noise level of the spectrum, the multidipole localization algorithm can find the locations of the overlapping activities.

The use of the single dipole model for the analysis of the data was only meaningful when one of the two sinusoidal varying dipole moments crossed the zero line. Therefore, at times when both dipoles are active, the estimated locations of the incorrectly assumed single dipole source do not coincide with any one of the correct positions. The estimated locations may lie between the two correct locations or they may lie at locations which are totally different from the region of both active sources (figure 2).

Real Data in Response to Somatosensory Stimulation

The evoked magnetic wave is presented as a blue waveform in the top panel of figure 3b. The red crosses in the MRI-sections of figure 3a mark locations for those time points at which the single dipole model results in an acceptable signal-to-noise ratio (6); corresponding time segments are colored in red in the time course of the evoked field. The best fit was achieved at 62 ms with a signal-to-noise ratio of 11.7. This point in time is marked with a gray bar.

The singular value spectrum (figure 4) indicates a clear

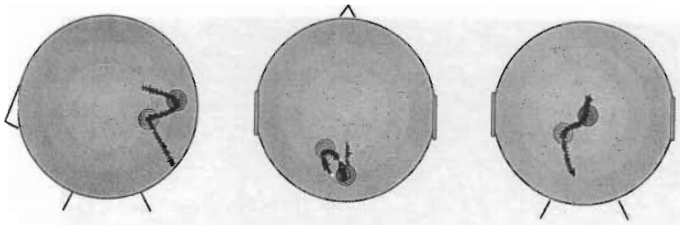

Figure 2. In a phantom model, two dipoles, fixed in location and orientation, have been activated with a sinusoidal amplitude. The phase between the sinusoidal currents was 90°. The true locations of the generators are indicated by circles. These locations correspond exactly to the locations identified by the described MUSIC-type approach. The single ECD only identifies correct positions for the instant of zero-crossing of the second generator. At other instances, the trajectory of the single ECD model (crosses) may be quite erratic.

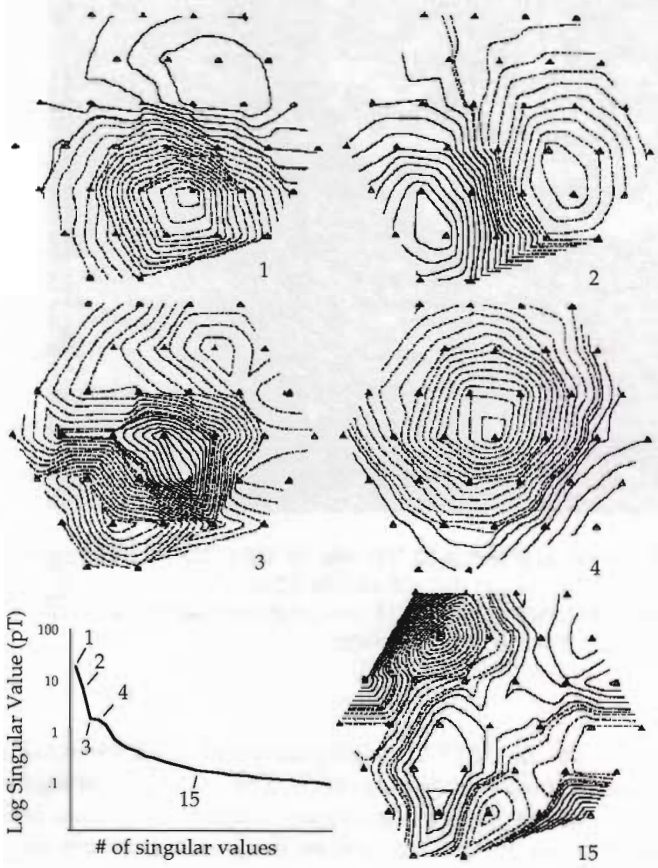

Figure 4. Singular value spectrum and eigenmaps for the somatosenory evoked field. Two large singular values which are related to S-I and S-II can be noted. Two to three additional values corresponding to ipsilateral, but also to the limited adequacy of the model applied (i.e., to further contralateral sources), might be considered. Correspondingly, the eigenmaps do not show a clear distinction between a source space and noise.

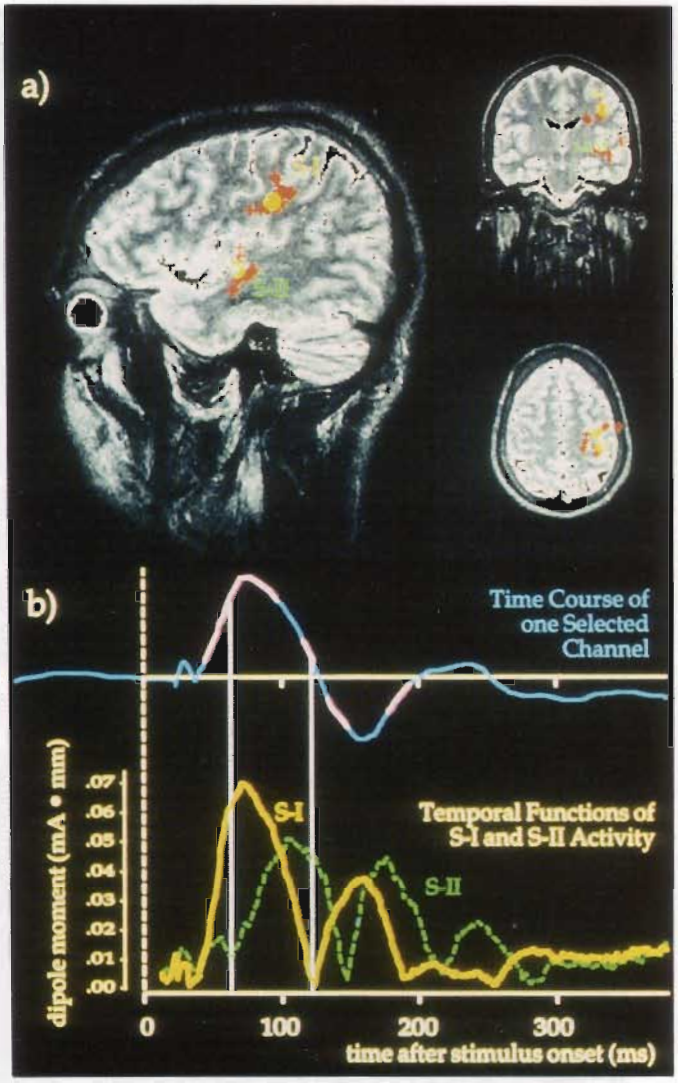

Figure 3a. Locations which result from the single moving ECD-model (red crosses) and from the MUSIC-like multi-dipole-dipole approach (circles) are superimposed onto MRI sections. Figure 3b. Evoked magnetic waveform (blue) of one selected MEG-channel. The red segments in the waveform correspond to a signal-to-noise ratio 6. The best fit was achieved at 62 ms with a signal-to-noise ratio of 11.7. This point in time is marked with a gray bar. The second gray bar, around 122 ms, corresponds to the best fit of ECD in the region of S-II. The bottom part illustrates the temporal development of two stationary sources assumed by the MUSIC-type approach, which turned out to correspond perfectly to S-I and S-II-regions.

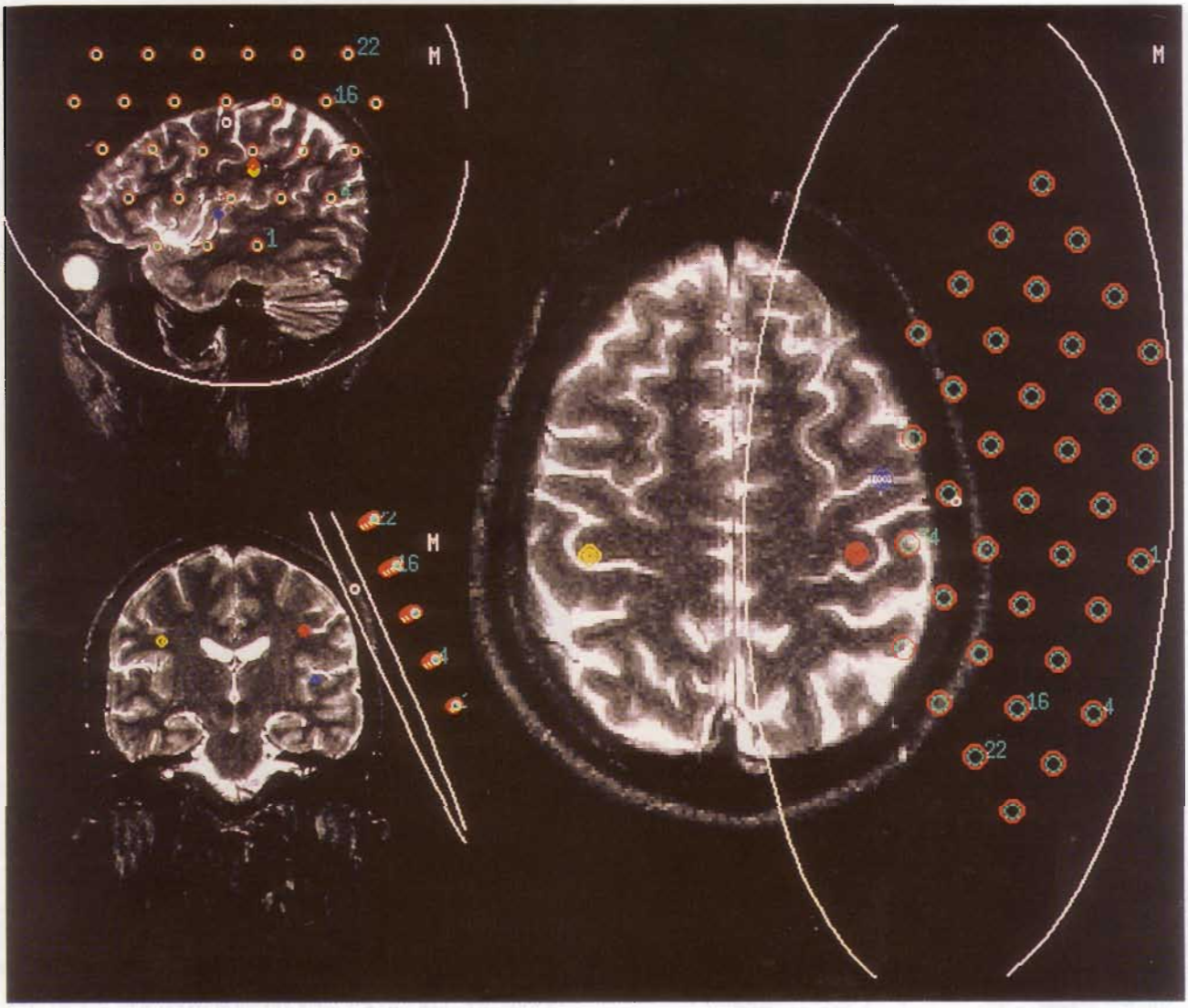

Figure 5. When the sensor array was positioned over the hemisphere ipsilateral to the site of stimulation, the present procedure identifies the S-I in both hemispheres (yellow and blue) and S-II on the ipsilateral side. The contralateral S-I location, obtained as a rather flat local maximum of a filtered weighted spatial function is in agreement with the locations derived from the measurements with the sensor array contralateral to the site of stimulation.

drop from the first to the second values, and again from the second to the third value. It then changes more gradually in a fashion characteristic for noise spectra. Only the first two to three eigenmaps show patterns clearly discernible from noise (figure 4). Based on the spectrum and eigenmaps it seems unclear whether two or three dipoles are active. In figure 3 only two activity components are considered to reflect the signal. The locations for these two dipoles, i.e., centers of activity, are marked by yellow and green circles. These locations correspond well with the expected regions of S-I and S-II but deviate from many of the locations suggested by the single ECD-model. There are, however, time points when the single ECD corresponds well with the results from the multi-dipole approach. The lower part of figure 3b illustrates the temporal development of both sources. Here it can be seen that instances do occur, where only one of the two sources is mainly active. From this we may conclude that the single dipole model may adequately depict the positions, when calculated during the upstroke of the first major component (in this particular case after 62 ms, marked by a grey bar). The best S-II fit may be obtained when the depolarization of S-I has already vanished while S-II is still active, (in the present case around 122 ms, marked by another gray bar).

Finally, figure 5 presents the results for the recording

ipsilateral to the stimulation. The location of the sensor is illustrated by the colored points. As can been seen, the described multi-dipole method depicts the location not only of the ipsilateral S-I and S-II responses but also of the contralateral S-I response, despite the fact that the dewar position was ipsilateral to the stimulation site. For this modeling, three overlapping dipole activities were suggested by the singular value analysis.

Discussion

In this work we evaluate phantom and somatosensory data with a recently developed multi-dipole localization algorithm. The algorithm allows multifocal activities, described as current dipoles, to be simultaneously active. In order to be able to disentangle the overlapping activities, these activities should evolve independently in time. Further assumptions or a priori information with respect to the number of sources, the regions of their locations or the kind (orientation and strength of the dipole moments) of the activities are not required. Thus, this localization procedure is more general than a source localization method based on a single ECD model. Results obtained with a single dipole search procedure are contained in the results of the localization method used.

As an example of a successful test of the algorithm we presented the evaluation of phantom data which were generated by two overlapping dipole activities. The locations and the activity patterns of these sources could be determined. It became evident that the single ECD model yields meaningful results if only one single source is active during the time interval under investigation. Therefore, if the number of focal sources is unknown, the analysis of the data with a multi-dipole search method is required. A single ECD model can be used to check the multi-dipole results if there are time segments with a single source being active. This has also been demonstrated.

The contra- and ipsilaterally measured somatosensory data could be explained in terms of two or three multifocal sources with overlapping activities, respectively. The number of sources was determined by inspection of the singular value spectra. This determination requires a sufficient signal-to-noise ratio in order to get a reliable estimate of the number of dipoles. Some a priori information would have been helpful but is, in principle, not necessary. For the contralateral data we expected to find two sources and did. However, in analyzing the ipsilateral measured data, it was unknown a priori how many sources could be found.

The interpretation of the data by means of narrowly localized activity centers may be too coarse a model of the real process. After an afferent volley has entered the cortical network, it is usually quickly distributed to various patches which itself vary in their activated size across time. There may be time instances when the sources can be well modeled by a single focal source, i.e., a dipole, or a polarized patch of cortical tissue (Lütkenhöner et al. 1995). However, it is not likely that all activity can be modeled by a set of stationary dipoles. Again, there are cases when such an assumption is reasonable, and where the described algorithm seems to work perfectly.

In the case of the contralateral data, time segments were found where only one source was active or was dominantly active, respectively. Thus, the source location could be again validated by the single ECD model.

The best single dipole estimates may be achieved during the upstroke of the large response component which appears in the 30-90 ms range. (The exact latency of this upstroke depends on the inter-stimulus-interval and the site of stimulation). This conclusion may be derived from the multidipole model which accounts for the separate activation in S-I and S-II. According to this model, after the short-latent components (not discussed in detail here) S-I is activated first, but S-II begins to contribute shortly after. As suggested by figure 3, the best time to locate the activity within S-I with a single ECD-model would be at 62 ms, where S-I activity is already high, but S-II is just beginning to rise. Later, at 122 ms, S-II is still active, but the S-I response has ceased (or is about to change its polarisation). When determined at these points, the ECD-model produces locations which correspond well to the ones suggested by the multidipole model.

The present waveforms can basically be explained as a depolarization-repolarization, with S-I preceding the same process in S-II. As far as we know, the only other attempt to describe the overlapping time course of S-I and S-II activity has been made by Hari et al. (1993). These authors used a model with two fixed dipoles and as a cross-validation the Mosher's MUSIC-algorithm to extract the temporal pattern of the two sources. Although the reported S-I response also shows two peaks, these are farther separated in time and the S-II response does not show a repolarization peak. However, as Hari et al. noted, the S-II response seem to vary considerably across subjects. In most of the somatosensory studies which we have performed (e.g., Elbert et al. 1994, 1995), we do not obtain satisfying single ECD-fits at or after the peak of the first major component (35-90 msec), but achieve excellent models during the upstroke of this component. This too would be in agreement with the assumption that S-II activation comes in only at stages beyond 50 msec, an assumption which is also consistent with the recent report by Buchner et al. (1994) showing that early SEFs (N20-P20) and N30-P30 peaks) can be

adequately modeled by a single ECD located close to the posterior bank of the central sulcus, in area 3b.

A further validation of the described Oppelt-Scholz procedure is its capability of correctly detecting the S-I response in the opposite hemisphere. Of course, the use of a gradiometer system with a large baseline (such as the presently used Siemens Krenikon with a baseline of 7 cm; for comparison, the BTI Magnes system uses 5 cm) is more favorable for the identification of sources in the opposite hemisphere. The results, however, suggest that with a small baseline sources from the hemisphere opposite to the sensors array influence the source modeling. For the somatosensory stimulation, this is even more true when responses from the trunk or leg are to be recorded.

The agreement of the localizations extracted from the ipsi- and contralateral sensor positions further validates the Oppelt-Scholz algorithm. This agreement is obtained despite the biological noise and the model error introduced by the simple spherical volume conductor model of the head. In this work, we analyzed biomagnetic data. It is, of course, possible to apply the Oppelt-Scholz algorithm to bioelectric data as well. In this case a more sophisticated volume conductor model for the head must be used.

References

Abraham-Fuchs, K., Strobach, P., Härer, W. and Schneider, S. Improvement of neuromagnetic localization by MCG-artifact correction in MEG recordings. In: M. Hoke, S.E. Erné, Y.C. Okada and G.L. Romani (Eds.), Biomagnetism: Clinical Aspects. Amsterdam: Excerpta Medica 1992, 787-792.

Buchner, H., Fuchs, M., Wischmann, H.-A., Dössel, O., Ludwig, I., Knepper, A. and Berg, P. Source analysis of median nerve and finger stimulated somatosensory evoked potentials: multichannel simultaneous recording of electric and magnetic fields combined with 3D-MR tomography. Brain Topography, 1994, 6: 299-310.

Elbert, T., Flor, H., N., B., Knecht, S., Hampson, S. and Taub, E. Extensive reorganization of the somatosensory cortex in adult humans after nervous system injury. Neuroreport, 1994, 5: 2593-2597.

Elbert T., Wienbruch, C., Pantev, C., Rockstroh, B. and Taub, E. Increased use of the left hand in string players associated with increased cortical representation of the fingers. Neuroreport, 1995, in press.

Hari, R., Karhu, J., Hämäläinen, M., Knuutila, J., Salonen, O., Sams, M. and Vilkman, V. Functional organization of the human first and second somatosensory cortices: a neuromagnetic study. European Journal of Neuroscience, 1993, 5: 724-734.

Hari, R., Karhu, J., Sams, M., Hämäläinen, M. and Knuutila, J. Magnetic responses reveal somatotopic organization of the second somatosensory cortex. In: M. Hoke, S.E. Erné, Y.C. Okada and G.L. Romani (Eds.), Biomagnetism: Clinical Aspects. Amsterdam: Excerpta Medica, 1992: 229-232.

Lawson, C.L. and Hanson, R.J. Solving least squares problems. Eaglewood Cliffs, N.J., USA, Prentice-Hall Inc., 1974.

Lütkenhöner, B. On the biomagnetic inverse prodecure's capability of separating two current dipoles with a priori known locations. In: M. Hoke, S.E. Erné, Y.C. Okada and G.L. Romani (Eds.), Biomagnetism: Clinical Aspects. Amsterdam: Excerpta Medica, 1992: 687-692.

Lütkenhöner, B., Lehnertz, K., Hoke, M. and Pantev, C. On the biomagnetic inverse problem in the case of multiple dipoles. Acta Oto-Laryngol. (Stockh.), 1991, Suppl. 491: 94-105.

Lütkenhöner, B., Menninghaus, E., Steinsträter, O., Wienbruch, C., Gißler H.M. and Elbert, T. Neuromagnetic source analysis using magnetic resonance images for the construction of source and volume conductor model. Brain Topography, 1995, (this volume).

Marshall, W.H., Woolsey, C.N. and Bard, P. Observations on cortical somatic sensory mechanisms of cat and monkey. J. Neurophysiol., 1941, 4: 1-24.

Mosher, J.C., Lewis, P.S. and Leahy, R.M. Multiple dipole modeling and localization from spatio-temporal MEG data. IEEE Trans Biomed Eng, 1992, 39: 541-57.

Oppelt, A., Graumann, R. and Scholz, B. Zur magnetischen Ortung bioelektrischer Quellen, Teil 1: Ortung einzelner und mehrerer Stromdipole. Z.Med.Phys., 1993, 2: 59-63.

Penfield, W. and Rasmussen, R. The Cerebral Cortex of Man. A Clinical Study of Localization of Function. New York: Macmillan, 1950.

Sarvas, J. Basic mathematical and electromagnetic concepts of the biomagnetic inverse problem. Phys. Med. Biol., 1987, 32: 11-22.

Scholz, B. and Oppelt, A. Probablility based dipole localization and individual error calculation in biomagnetism. Proc. of the 14th Annual International Conference of the IEEE Engineering in Medicine and Biology Soc., Vol. 5, 1766, 1992.

Scholz, B. and Oppelt, A. On multiple source localization from spatio-temporal biomagnetic data. Physics in Medicine and Biology, 1995, in press.

Schneider, S., Hoenig, E., Reichenberger, H., Abraham-Fuchs, K., Moshage, W., Oppelt, A., Stefan, H., Weikl, A. and Wirth, A. A multichannel biomagnetic system for study of electrical activity in the brain and heart. Radiology, 1990, 176:825-830.

Yang, T.T., Gallen, C.C., Schwartz, B.J. and Bloom, F.E. Noninvasive somatosensory homunculus mapping in humans by using a large-array biomagnetometer. Proc. Natl. Acad. Sci., 1993, 90: 3089-3102.